Mesoporous single-crystal Co_3O_4 templated by cage-containing mesoporous silica

Wenbo Yue,[a] Adrian H. Hill,[b] Andrew Harrison[bc] and Wuzong Zhou*[a]

Received (in Cambridge, UK) 5th January 2007, Accepted 21st February 2007
First published as an Advance Article on the web 15th March 2007
DOI: 10.1039/b700185a

Mesoporous single-crystal Co_3O_4 was obtained using cage-containing mesoporous silicas, FDU-12 and SBA-16, as templates and characterised by XRD, HRTEM and nitrogen adsorption–desorption while SQUID magnetometry was used to probe the magnetic character.

In our previous papers and the reports from others,[1–5] it has been demonstrated that crystal growth of transition metal oxides inside the pores of mesoporous silica, SBA-15 and KIT-6, leads to mesoporous single-crystal oxides, which may be developed into new forms of catalysts with high activity and selectivity, and new materials with some interesting physical properties. The porous oxides produced can be regarded as negative replicas of the mesoporous silicas and, therefore, the morphology of the building unit has the same shape of the original pores in the silica template. Both the pore structures of SBA-15[6] and KIT-6[7] contain cylindrical pore units. As a result, the building unit in the porous crystals of oxides templated by them is a piece of nanorod. In SBA-15, some small subchannels connecting the principal channels must be available for crystal expansion. Otherwise, individual nanowires instead of three dimensional porous crystals are produced.[8]

Unlike the formation of mesoporous silicas, where the silicate species and surfactant molecules may aggregate simultaneously,[9] the hard templates are prepared first for the porous metal oxides. Therefore, an important step is to impregnate the templating pores with the precursor. This can be achieved in different ways. In the first method, the inner surface of mesoporous silica is functionised *via* aminosilylation of the silanols and then anchoring the acidic precursor (*e.g.* $H_2Cr_2O_7$, $H_3PW_{12}O_{40}$) molecules.[1] The second method is the so-called "two solvents" impregnation method. For example, a suspension of mesoporous silica in dry hexane is mixed with an aqueous solution of metal nitrate. The precursor molecules will then move into the pores during a stirring.[2] Recently, some porous crystals of oxides were fabricated *via* an evaporation method, *i.e.* simply dissolving the nitrate precursor in ethanol. It was expected that the precursor molecules would enter the pores during the evaporation of ethanol by a capillary action.[3] The impregnation can also be achieved by a solid-state grinding route if a suitable precursor is used.[10] In the present work, we synthesized porous Co_3O_4 crystals by using this latter method and using some cage-containing mesoporous silicas as templates.

[a]*School of Chemistry, University of St. Andrews, St. Andrews, Fife, UK KY16 9ST. E-mail: wzhou@st-andrews.ac.uk; Fax: +44 (0)1334 463808; Tel: +44 (0)1334 467276*
[b]*School of Chemistry and EaStChem, The University of Edinburgh, The King's Buildings, West Mains Rd., Edinburgh, UK EH9 3JJ*
[c]*Institut Laue-Langevin, 6, rue Jules Horowitz BP, 156 - 38042, Grenoble, France*

Co_3O_4 has potential applications[11] in electrochromic devices, gas sensors, Li-ion rechargeable battery, semiconductors, solar energy absorbers and heterogeneous catalysts. Mesoporous Co_3O_4 crystals may have improved properties for these applications because of their large specific surface areas and shape selectivity.

Both SBA-16[12] and FDU-12[13] have mesoporous networks built by spherical nanocages connected by some windows. SBA-16 has a body-centred cubic structure (space group $Im\bar{3}m$) and FDU-12 is face-centred cubic (space group $Fm\bar{3}m$). Accordingly, each spherical nanocage is 8 coordinated by the neighbouring nanocages in SBA-16, but 12 coordinated in FDU-12. When porous crystals of Co_3O_4 form in these two silica phases, we expect the structures of the products to be three dimensional arrangements of solid nanospheres connected to each other by some very short nanorods as shown in Fig. 1.

SBA-16 and FDU-12 were synthesized according to the established methods.[12,13] For FDU-12, the windows connecting the spherical nanocages could be tuned from 4 to 7.5 nm while the change of diameter of the nanocages was not so significant (from 10 to 12 nm), mainly by changing the maturing temperature.[13] In the present work, the hydrothermal conditions of 100 °C for small windows (4 nm) were selected. The metal oxide $Co(NO_3)_3{\cdot}6H_2O$ was impregnated within the mesoporous silica using a solid–liquid method. 1 mmol of $Co(NO_3)_3{\cdot}6H_2O$ was mixed with 0.15 g of SBA-16 or FDU-12, and was ground for a few minutes. The mixture was then placed in a crucible and heated in a muffle furnace. The temperature was increased slowly (1 °C min^{-1}) from room temperature up to 500 °C. The specimen was kept at 500 °C for 5 h before cooling down.

In this method, a mixture of two solids was heated directly without using any solvent. The essential condition for this method is that the melting point of $Co(NO_3)_2{\cdot}6H_2O$ (55 °C) is lower than its decomposition temperature (74 °C). When $Co(NO_3)_2{\cdot}6H_2O$ melted at 55 °C, the liquid phase covered the external surface of

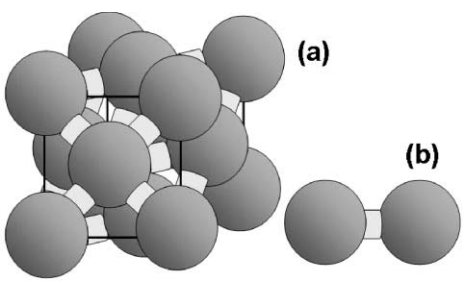

Fig. 1 (a) Expected structure of porous crystals of Co_3O_4 templated by FDU-12. (b) The basic building unit in (a) which is also the same in the porous crystals templated by SBA-16.

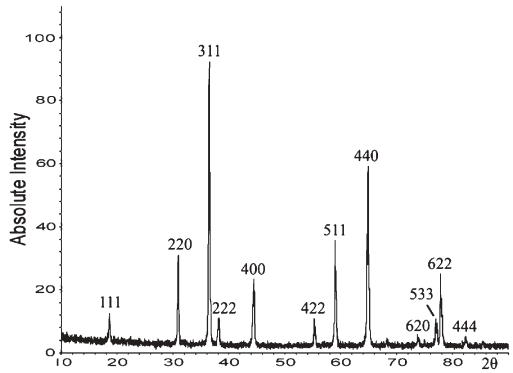

Fig. 2 XRD pattern of porous Co_3O_4 crystals templated by SBA-16, indexed onto the cubic unit cell with a = 0.8085 nm.

the silica particles and moved into the pores under capillary action. The precursor was then decomposed step by step with increasing temperature, forming intermediate compounds, such as $Co(NO_3)_2 \cdot 2H_2O$ by losing $4H_2O$, and $Co(NO_3)(OH) \cdot H_2O$ by further losing HNO_3. Crystalline Co_3O_4 formed at the final stage. This process is different from one outside the mesopores due to a confinement effect. The silica template was then removed with a 10 wt% HF aqueous solution. A black powder product of mesoporous Co_3O_4 crystals was obtained by centrifugation and washed with distilled water thrice.

Initial characterisation of the specimens was by X-ray powder diffraction (XRD). Both XRD patterns of the cobalt oxides templated by SBA-16 and FDU-12 indicate that the products are cubic Co_3O_4, space group $Fd\bar{3}m$ (Fig. 2).

Further investigation of the products was carried out by selected area electron diffraction (SAED), transmission electron microscopy (TEM) and high resolution TEM (HRTEM) on JEOL-JEM-2011 microscope operated at 200 kV. Fig. 3a shows a TEM image of a FDU-12 particle whose spherical cavities have been partially filled with Co_3O_4 crystals (the dark areas). The size of these particles is variable. For example, the particle in the centre of Fig. 3a is about 150 nm in diameter, while at the top right corner, there is a much larger particle. The silica particles cannot be entirely filled by Co_3O_4, because even it is fully filled at beginning by $Co(NO_3)_2 \cdot 6H_2O$, the volume of the cobalt compound will be significantly reduced when it decomposes and forms Co_3O_4.

Fig. 3b shows porous Co_3O_4 crystals after the template was removed. The pore system in FDU-12 has been replicated by the metal oxide. The diameter of the main particle is about 600 nm and some small particles nearby are only about 100 nm in diameter.

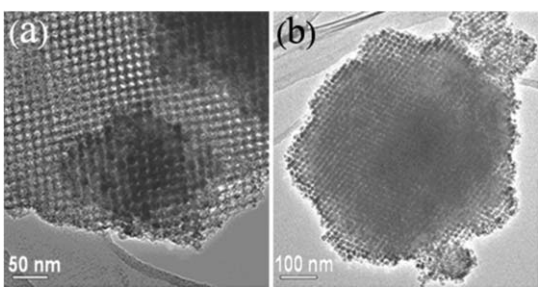

Fig. 3 (a) TEM image of a particle of FDU-12 containing some cobalt oxide nanospheres. (b) Porous cobalt oxide crystals after removing the silica template.

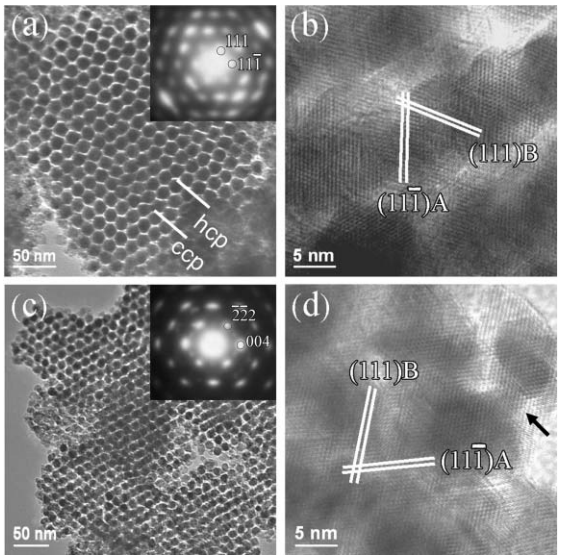

Fig. 4 TEM images of porous Co_3O_4 templated by (a) FDU-12 and (c) SBA-16. In (a), irregular intergrowth of ccp and hcp stackings is indicated. The insets in (a) and (c) are SAED patterns from these two samples of crystalline Co_3O_4. (b) and (d) HRTEM images of Co_3O_4 templated by FDU-12 and SBA-16, respectively. The arrow in (d) points to the bridge connecting two nanospheres. The d-spacings of the marked fringes are *ca.* 0.467 nm, corresponding to the {111} planes of Co_3O_4.

The chemical composition of the specimen was examined by energy dispersive X-ray spectroscopy (EDX). The EDX spectra from cobalt oxide with the FDU-12 template show the elements cobalt, oxygen and silicon. After the template was dissolved, no silicon was present in the samples.

TEM images with higher magnifications of the porous Co_3O_4 crystals templated by FDU-12 and SBA-16 (Fig. 4) indicated that the porous crystals were both made of nanoballs connected by nanobridges. Such bridges can be observed at the edge of the particles as indicated by an arrow in Fig. 4(d). In the FDU-12 templated Co_3O_4, the nanospheres are in a cubic close packed arrangement and some stacking faults, also commonly seen in FDU-12, namely irregular intergrowth of cubic close-packing (ccp) and hexagonal close-packing (hcp), are often observed. In the SBA-16 templated porous oxide, the nanospheres are in a body centred arrangement and such defects do not form.

SAED patterns from large areas show the single-crystal property and can be indexed to the cubic Co_3O_4 structure, as shown in the insets in Fig. 4 (a) and (c). HRTEM images of the porous Co_3O_4 crystals further confirm the single-crystal property (Fig. 4(b) and (d)). Since the crystal orientation of Co_3O_4 has no relation with the orientation of the mesopore network, it is difficult to find a viewing direction parallel to a principal orientation in both the Co_3O_4 crystal and the mesopore system. Consequently, when we found a good projection for the mesopore network, *e.g.* shown in Fig. 4(a) and (c), we missed a principal crystal orientation of Co_3O_4. Similarly, when we approached a principal orientation of the crystal as shown in Fig. 4(b) and (d), the arrangement of the nanospheres could not be clearly revealed.

Fig. 5 shows the nitrogen adsorption–desorption isotherms of the porous Co_3O_4 products. The isotherms of Co_3O_4 porous crystals are both type IV with a hysteresis loop, indicating the mesoporous property. The specific surface areas of Co_3O_4 crystals

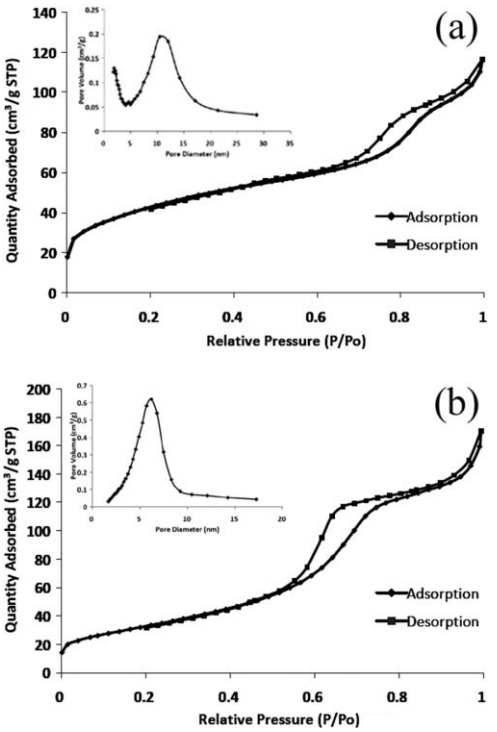

Fig. 5 Nitrogen adsorption–desorption isotherms measured at 77 K from porous crystals of Co_3O_4 templated by (a) FDU-12 and (b) SBA-16. Insets: pore size distribution of the corresponding crystals.

templated by FDU-12 and SBA-16 are 151(1) and 122.4(6) $m^2\ g^{-1}$, respectively, which are larger than the surface area of Co_3O_4 templated by KIT-6 (92 $m^2\ g^{-1}$).[3] For a comparison with the surface areas in FDU-12 (410 $m^2\ cm^{-3}$) and in SBA-16 (686 $m^2\ cm^{-3}$), the above values were altered to 450 (FDU-12 templated, pore volume is 0.171 $cm^3\ g^{-1}$) and 298 $m^2\ cm^{-3}$ (SBA-16 templated, pore volume is 0.246 $cm^3\ g^{-1}$) when the densities of 2.2 g cm^{-3} (SiO_2) and 6.07 g cm^{-3} (Co_3O_4) were used. The diameters of the nanospheres in these two specimens are similar as seen in Fig. 4. and the average pore size of the SBA-16 templated Co_3O_4 (6.6 nm) is slightly larger than that in the FDU-12 templated sample (6.1 nm). The large specific surface areas in the samples also indicate high yields.

Finally, preliminary magnetic characterisation of a Co_3O_4 sample templated with SBA-16 was performed by SQUID magnetometry. Measurements were made from 2–340 K in 0.01 T after cooling to base temperature in zero field. The temperature-dependent susceptibility and effective magnetic moment are displayed in Fig. 6, revealing behaviour similar to that seen in bulk Co_3O_4 (Aldrich, 99.995%). The results of the measurements on the bulk material are displayed in the same figure for comparison, and these observations and interpretation may also be compared with those of similar work on another form of mesoporous Co_3O_4.[14]

WZ thanks St Andrews University for an EaStCHEM studentship for WY and AH thanks the University of Edinburgh for a studentship for AHH.

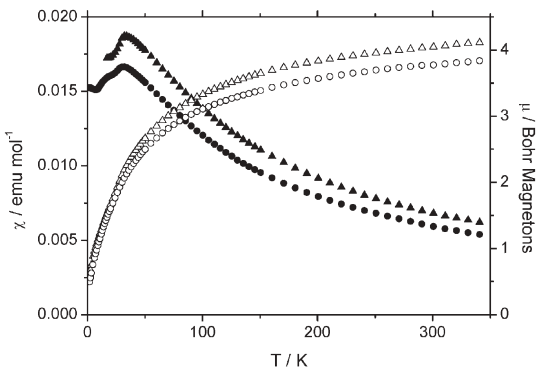

Fig. 6 Temperature dependence of magnetic susceptibility (solid circles) and effective magnetic moment (open circles) of Co_3O_4 templated by SBA-16 and measured in 0.01 T after cooling to base temperature in zero field. The behaviour of bulk Co_3O_4 is depicted by triangles—open and closed as for the mesoporous form.

Notes and references

1 K. K. Zhu, B. Yue, W. Z. Zhou and H. Y. He, *Chem. Commun.*, 2003, 98; B. Yue, H. L. Tang, Z. P. Kong, K. K. Zhu, C. Dickinson, W. Z. Zhou and H. Y. He, *Chem. Phys. Lett.*, 2005, **407**, 83.
2 K. Jiao, B. Zhang, B. Yue, Y. Ren, S. X. Liu, S. R. Yan, C. Dickinson, W. Z. Zhou and H. Y. He, *Chem. Commun.*, 2005, 5618.
3 C. Dickinson, W. Z. Zhou, R. P. Hodgkins, Y. F. Shi, D. Y. Zhao and H. Y. He, *Chem. Mater.*, 2006, **18**, 3088.
4 B. Z. Tian, X. Y. Liu, H. F. Yang, S. H. Xie, C. Z. Yu, B. Tu and D. Y. Zhao, *Adv. Mater.*, 2003, **15**, 1370; B. Z. Tian, X. Y. Liu, L. A. Solovyov, Z. Liu, H. F. Yang, Z. D. Zhang, S. H. Xie, F. Q. Zhang, B. Tu, C. Z. Yu, O. Terasaki and D. Y. Zhao, *J. Am. Chem. Soc.*, 2004, **126**, 865.
5 F. Jiao, A. Harrison, J. C. Jumas, A. V. Chadwick, W. Kockelmann and P. G. Bruce, *J. Am. Chem. Soc.*, 2006, **128**, 5468.
6 D. Y. Zhao, J. L. Feng, Q. S. Huo, N. Melosh, G. H. Fredrickson, B. F. Chmelka and G. D. Stucky, *Science*, 1998, **279**, 548.
7 F. Kleitz, S. H. Choi and R. Ryoo, *Chem. Commun.*, 2003, 2136.
8 K. K. Zhu, H. Y. He, S. H. Xie, X. A. Zhang, W. Z. Zhou, S. L. Jin and B. Yue, *Chem. Phys. Lett.*, 2003, **377**, 317.
9 C. F. Cheng, H. Y. He, W. Z. Zhou and J. Klinowski, *Chem. Phys. Lett.*, 1995, **244**, 117; W. Z. Zhou and J. Klinowski, *Chem. Phys. Lett.*, 1998, **292**, 207.
10 Y. M. Wang, Z. Y. Wu, H. J. Wang and J. H. Zhu, *Adv. Funct. Mater.*, 2006, **16**, 2374.
11 F. Švegl, B. Orel and M. Hutchins, *J. Sol-Gel Sci. Technol.*, 1997, **8**, 765; W. Y. Li, L. N. Xu and J. Chen, *Adv. Funct. Mater.*, 2005, **15**, 851; J. Wollenstein, M. Burgmair, G. Plescher, T. Sulima, J. Hildenbrand, H. Bottner and I. Eisele, *Sens. Actuators, B*, 2003, **93**, 442; P. Poizot, S. Laruelle, S. Grugeon, L. Dupont and J. M. Tarascon, *Nature*, 2000, **407**, 496; S. A. Needham, G. X. Wang, K. Konstantinov, Y. Tournayre, Z. Lao and H. K. Liu, *Electrochem. Solid State Lett.*, 2006, **9**, A315; C. S. Cheng, M. Serizawa, H. Sakata and T. Hirayama, *Mater. Chem. Phys.*, 1998, **53**, 225; A. G. Avila, E. C. Barrera, L. A. Huerta and S. Muhl, *Sol. Energy Mater. Sol. Cells*, 2004, **82**, 269; D. Mehandjiev and E. Nikolovazhecheva, *J. Catal.*, 1980, **65**, 475; L. Yan, X. M. Zhang, T. Ren, H. P. Zhang, X. L. Wang and J. S. Suo, *Chem. Commun.*, 2002, 860.
12 D. Y. Zhao, Q. S. Huo, J. L. Feng, B. F. Chmelka and G. D. Stucky, *J. Am. Chem. Soc.*, 1998, **120**, 6024.
13 J. Fan, C. Z. Yu, F. Gao, J. Lei, B. Z. Tian, L. M. Wang, Q. Luo, B. Tu, W. Z. Zhou and D. Y. Zhao, *Angew. Chem., Int. Ed.*, 2003, **42**, 3146; J. Fan, C. Z. Yu, J. Lei, Q. Zhang, T. C. Li, B. Tu, W. Z. Zhou and D. Y. Zhao, *J. Am. Chem. Soc.*, 2005, **127**, 10794.
14 Y. Q. Wang, C. M. Yang, W. Schmidt, B. Spliethoff, E. Bill and F. Schuth, *Adv. Mater.*, 2005, **17**, 53.

